Appendix: NMA All Results

Search string

Ovid MEDLINE(R) Epub Ahead of Print, In Process & Other Non-Indexed Citations, Ovid MEDLINE (R) Daily, and Ovid MEDLINE (R) 1946-Present

1 Laparoscopy/ or laparoscopy.mp.
2 Minimally Invasive Surgical Procedures/ or minimal* invas*.mp.
3 Robotic Surgical Procedures/ or Robot* surg*.mp.
4 Pancreaticoduodenectomy.mp. or Pancreaticoduodenectomy/
5 Pancreaticoduodenectomy/
6 Whipple.mp.
7 pancrea* surg*.mp.
8 pancrea* resect*.mp.
9 1 or 2 or 3
10 4 or 5 or 6 or 7 or 8
11 9 and 10
12 limit 11 to (clinical trial, all or clinical trial or randomized controlled trial)

Embase <1980 to 2024 May 23>

1 laparoscopic surgery/ or laparscop*.mp.
2 minimally invasive surgery/ or minimal* invas*.mp.
3 robot assisted surgery/ or robot* surg*.mp. or robotic surgery/
4 Pancreaticoduodenectomy.mp. or pancreaticoduodenectomy/
5 pancreatoduodenectomy.mp.
6 Whipple.mp.
7 pancreas resection/ or pancrea* resection.mp.
8 pancreas surgery/ or pancrea* surg*.mp.
9 1 or 2 or 3
10 4 or 5 or 6 or 7 or 8
11 9 and 10
12 limit 11 to (clinical trial or randomized controlled trial or controlled clinical trial or multicenter study or phase 1 clinical trial or phase 2 clinical trial or phase 3 clinical trial or phase 4 clinical trial)

Central

ID Search Hits
#1 (laparascop*):ti,ab,kw (Word variations have been searched)
#2 MeSH descriptor: [Minimally Invasive Surgical Procedures] explode all trees
#3 MeSH descriptor: [Robotic Surgical Procedures] explode all trees
#4 MeSH descriptor: [Pancreaticoduodenectomy] explode all trees
#5 (pancrea* resection):ti,ab,kw (Word variations have been searched)
#6 (pancrea* surger*):ti,ab,kw (Word variations have been searched)
#7 #1 OR #2 OR #3
#8 #4 OR #5 OR #6
#9 #7 AND #8

#10 surger*
#11 operation*
#12 resection*
#13 #10 OR #11 OR #12
#14 #7 AND #8 AND #13

Supplementary methods

R (R Foundation for Statistical Computing, Vienna, Austria) was used for this analysis using the *meta* package. In studies that reported medians for continuous variables, mean and standard deviation estimates were calculated from the methods of Wan et al. and Luo et al(1,2). We first conducted a random-effects meta-analysis for primary outcomes. The relative risk (RR) and 95% confidence interval (95% CI) were estimated.

Subsequently we performed a trial sequential analysis (TSA) to assess the reliability of the effect size based on cumulative aggregation of included trials per the recommendations of Pogue and Yusuf (3). If corrected trial sequential monitoring boundaries were crossed prior to meeting the required information size, meta-analyses were considered reliable, and if not, further RCTs are required. To mitigate the increased risk of type I error due to repeated significance testing in meta-analyses, we followed Pogue and Yusuf's recommendation to construct Kim-DeMets sequential monitoring boundaries tailored for meta-analyses. Information size (IS) was estimated taking into account heterogeneity of included trials, treatment effect, control group event rate and desired type I error. Trial sequential monitoring boundaries (TSMBs) corrected for heterogeneity, helping guard against false positive results. We calculated the required information size (RIS) with predefined alpha and beta errors. Crossing TSMB before RIS suggests a reliable result of the meta-analysis. However, if this were not the case, further RCTs are required for validation of the hypotheses.

A random-effects network meta-analysis (NMA) was performed using GeMTC in R (4). GeMTC employs a Bayesian framework with non-informative priors. Network maps were generated to visualise all direct comparisons made. Line thickness corresponded with the number of studies assessing a particular direct comparison and the size of nodes correlated with the number of participants receiving a particular intervention. Odds ratios (OR) were used for categorical outcome data, and mean differences (MD) for continuous data, both accompanied by 95 per cent credibility intervals (cr.i.). Open pancreaticoduodenectomy was the comparator arm. Rankogram plots visualised the relative effectiveness of each intervention per outcome represented as stacked bar plots of the probability of each intervention achieving each rank. Sum under the cumulative ranking scores were used to rank interventions where a score of 1 meant the intervention was the best ranked 100 per cent of the time, and a score of 0 where it ranked as the worst intervention 100 percent of the time (5). Heterogeneity was assessed by assessing the random-effects standard deviations (6). Transitivity was assessed by collecting and comparing demographic data, surgical approach and co-interventions across direct comparisons. Comparison-adjusted funnel plots were constructed and visually inspected for asymmetry to indicate publication bias.

References

1. Wan X, Wang W, Liu J, Tong T. Estimating the sample mean and standard deviation from the sample size, median, range and/or interquartile range. BMC Med Res Methodol. 2014 Dec 19;14:135.

2. Luo D, Wan X, Liu J, Tong T. Optimally estimating the sample mean from the sample size, median, mid-range, and/or mid-quartile range. Stat Methods Med Res. 2018 Jun;27(6):1785–805.

3. Pogue JM, Yusuf S. Cumulating evidence from randomized trials: utilizing sequential monitoring boundaries for cumulative meta-analysis. Control Clin Trials. 1997 Dec;18(6):580–93; discussion 661–6.

4. Krieder SJ, Wozniak JM, Armstrong T, Wilde M, Katz DS, Grimmer B, et al. Design and evaluation of the gemtc framework for GPU-enabled many-task computing. In: Proceedings of the 23rd international symposium on High-performance parallel and distributed computing. New York, NY, USA: Association for Computing Machinery; 2014. p. 153–64. (HPDC ’14).

5. Salanti G, Ades AE, Ioannidis JPA. Graphical methods and numerical summaries for presenting results from multiple-treatment meta-analysis: an overview and tutorial. J Clin Epidemiol. 2011 Feb;64(2):163–71.

6. de Keijser J van VGBSEORDSC. gemtc.drugis.org. Available from: https://gemtc.drugis.org/signin.html#!/analyses 2016

Risk of Bias Assessment

Supplementary figure 1.Bar-chart of overall risk of bias

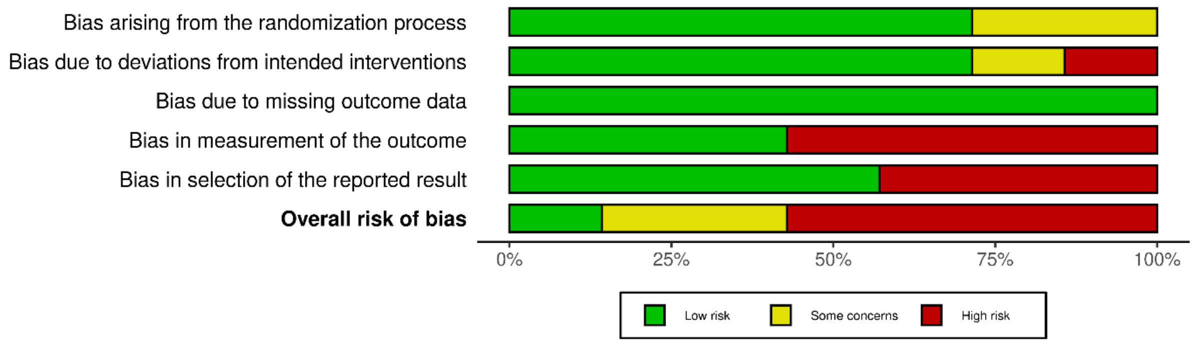

Supplementary figure 2. Risk of bias by domains

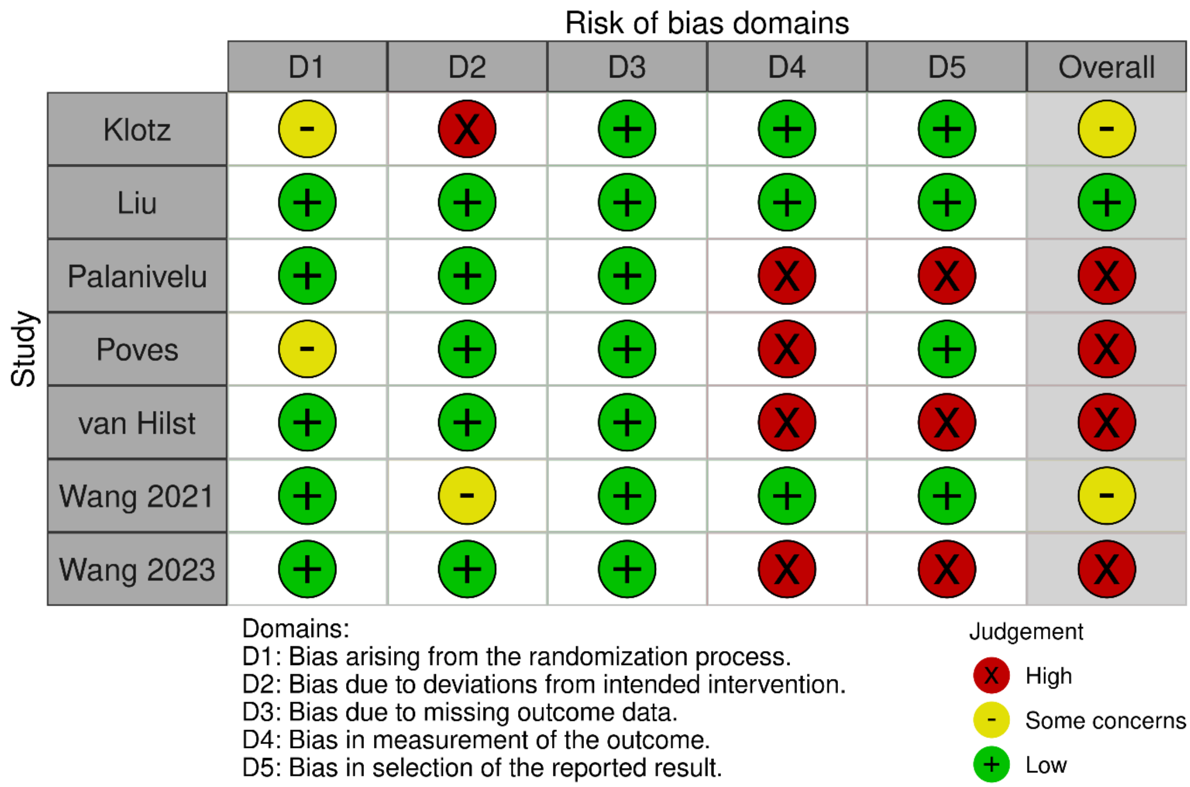

Network meta-analysis

Length of stay

Figure 3. Network graph for length of stay

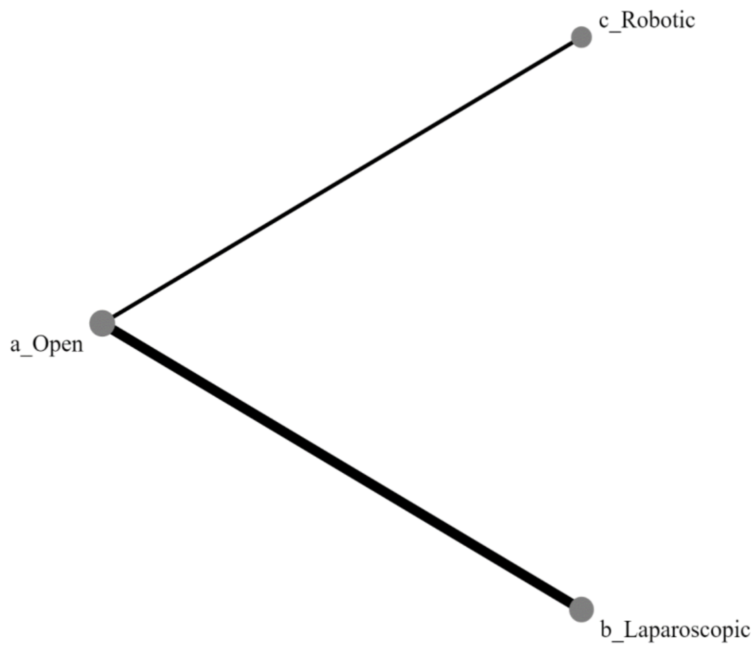

Table 2. Comparison of the included interventions: mean difference (95% CrI). Each cell gives the effect of the column-defining intervention relative to the row-defining intervention.

a_Open	-1.650 (-5.984, 0.906)	0.307 (-3.735, 6.544)
	b_Laparoscopic	1.970 (-2.320, 10.160)
		c_Robotic

Figure 4. Forest plot for length of stay

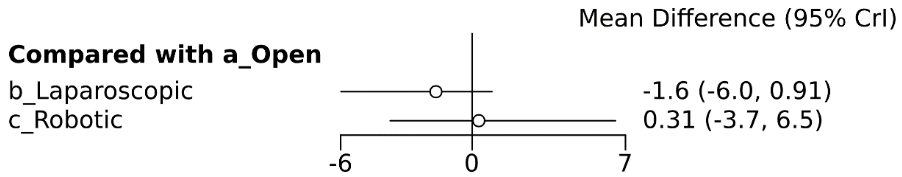

Table 3. Rank probabilities table

	Rank 1	Rank 2	Rank 3
a_Open	0.040	0.554	0.405
b_Laparoscopic	0.826	0.145	0.029
c_Robotic	0.133	0.301	0.566

Figure 5. Rankogram for Length of stay

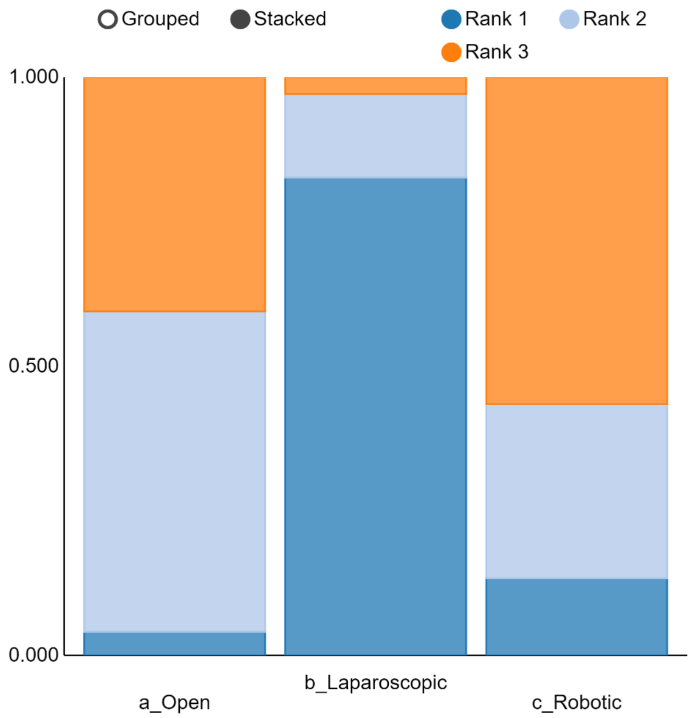

90-day Mortality

Figure 6. Network graph for 90-mortality

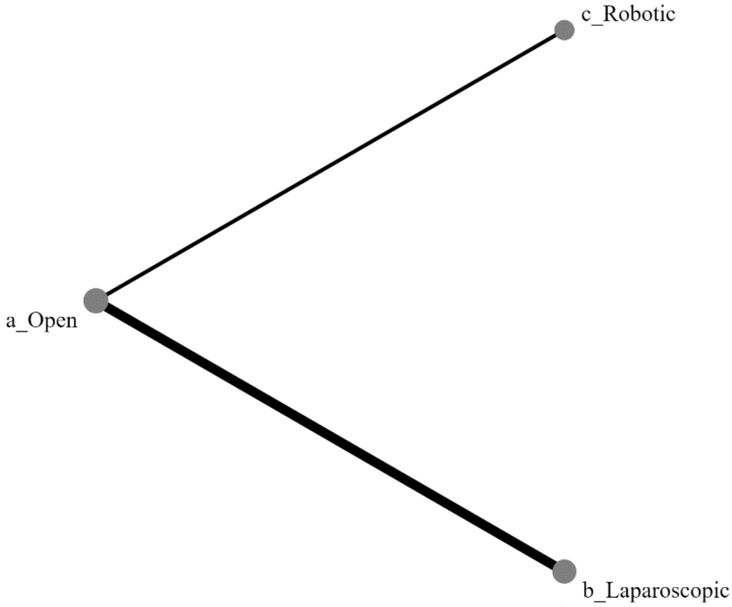

Table 4. Comparison of the included interventions: odds ratio (95% CrI). Each cell gives the effect of the column-defining intervention relative to the row-defining intervention.

a_Open	1.590 (0.312, 7.995)	0.169 (0.003, 3.147)
	b_Laparoscopic	0.103 (0.001, 2.796)
		c_Robotic

Figure 7. Forest plot for 90-mortality

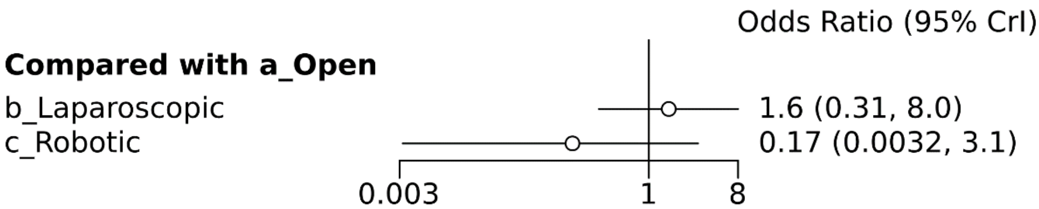

Table 5. Rank probabilities table

	Rank 1	Rank 2	Rank 3
a_Open	0.081	0.694	0.225
b_Laparoscopic	0.054	0.235	0.711
c_Robotic	0.866	0.071	0.064

Figure 8. Rankogram for 90-mortality

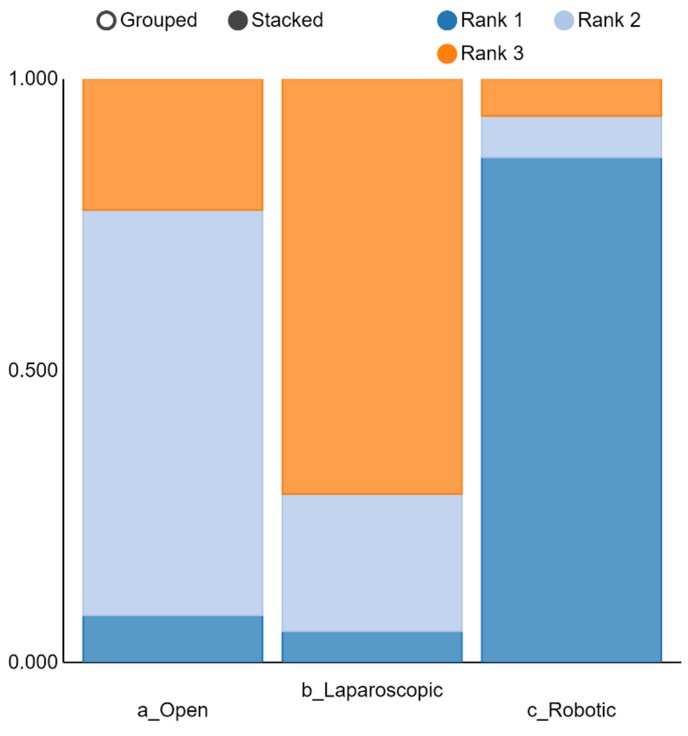

90-day Readmission

Figure 10. Network graph for 90-readmission

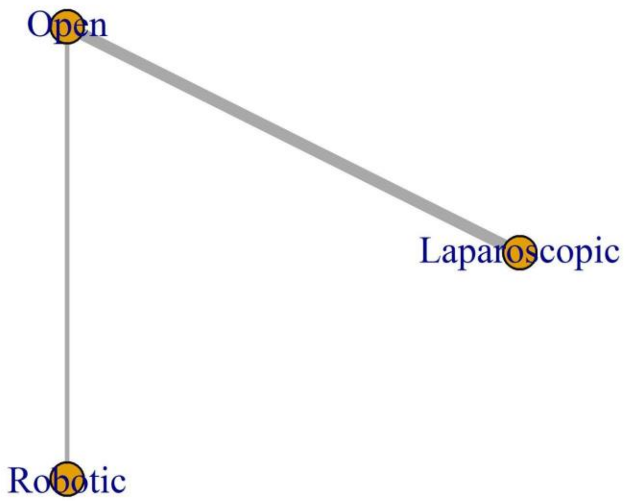

Table 6. Comparison of the included interventions: odds ratio (95% CrI). Each cell gives the effect of the column-defining intervention relative to the row-defining intervention.

a_Open	1.001 (0.441, 2.623)	1.178 (0.320, 4.458)
	b_Laparoscopic	1.172 (0.260, 6.295)
		c_Robotic

Figure 11. Forest plot for 90-readmission

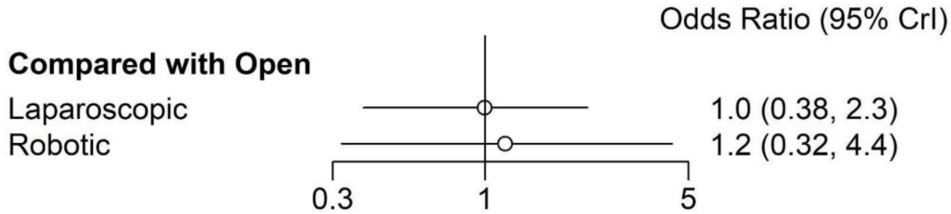

Table 7. Rank probabilities table

	Rank 1	Rank 2	Rank 3
a_Open	0.304	0.495	0.201
b_Laparoscopic	0.381	0.323	0.296
c_Robotic	0.314	0.183	0.503

Figure 12. Rankogram for 90-readmission

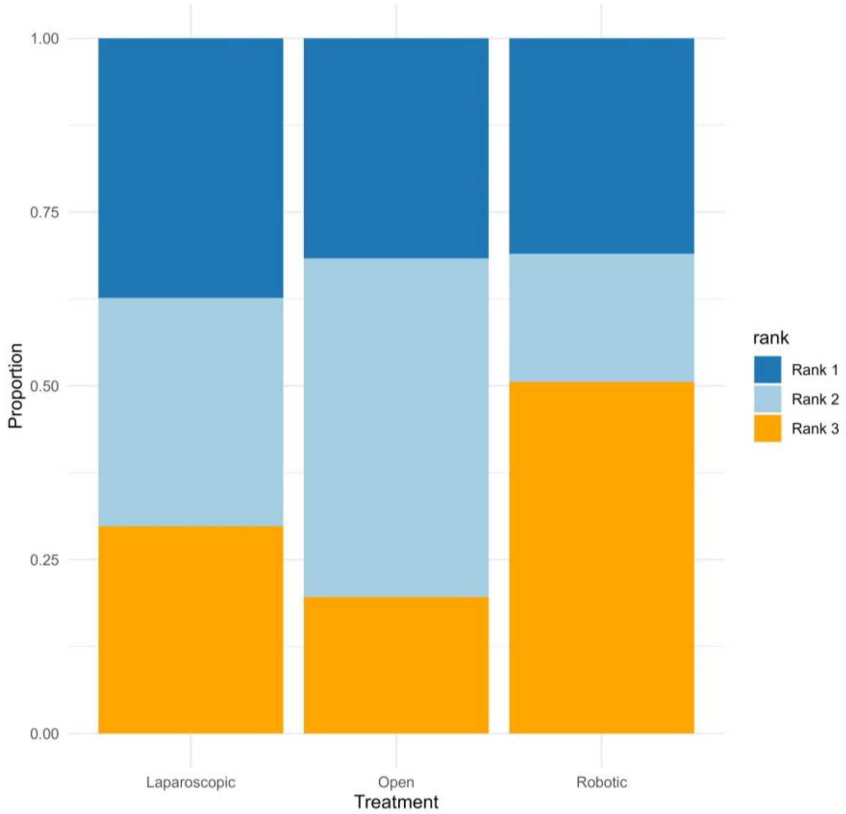

90-day reoperation

Figure 13. Network graph for 90-reoperation

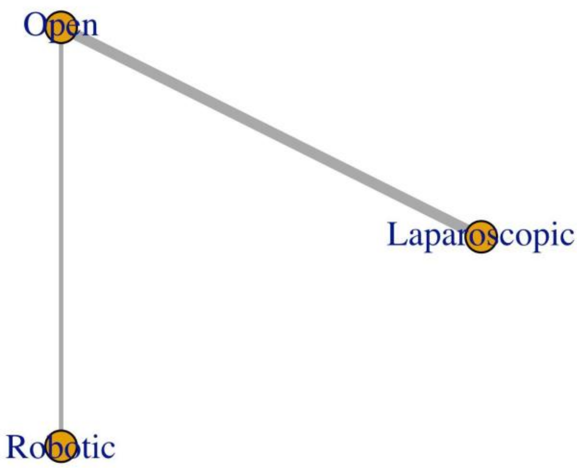

Table 8. Comparison of the included interventions: odds ratio (95% CrI). Each cell gives the effect of the column-defining intervention relative to the row-defining intervention.

a_Open	1.081 (0.422, 2.933)	0.744 (0.151, 3.472)
	b_Laparoscopic	0.813 (0.128, 5.035)
		c_Robotic

Figure 14. forrest plot for 90-reoperation

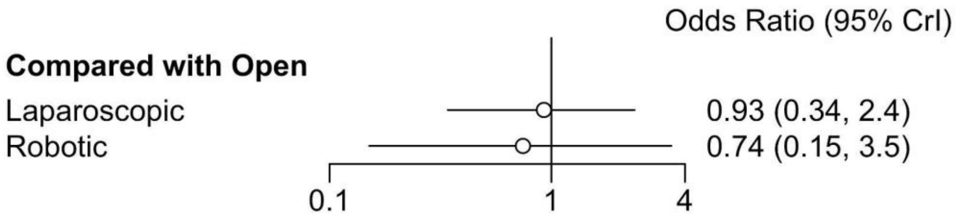

Table 9. Rank probabilities table

	Rank 1	Rank 2	Rank 3
a_Open	0.147	0.474	0.380
b_Laparoscopic	0.307	0.355	0.337
c_Robotic	0.545	0.172	0.283

Figure 15.

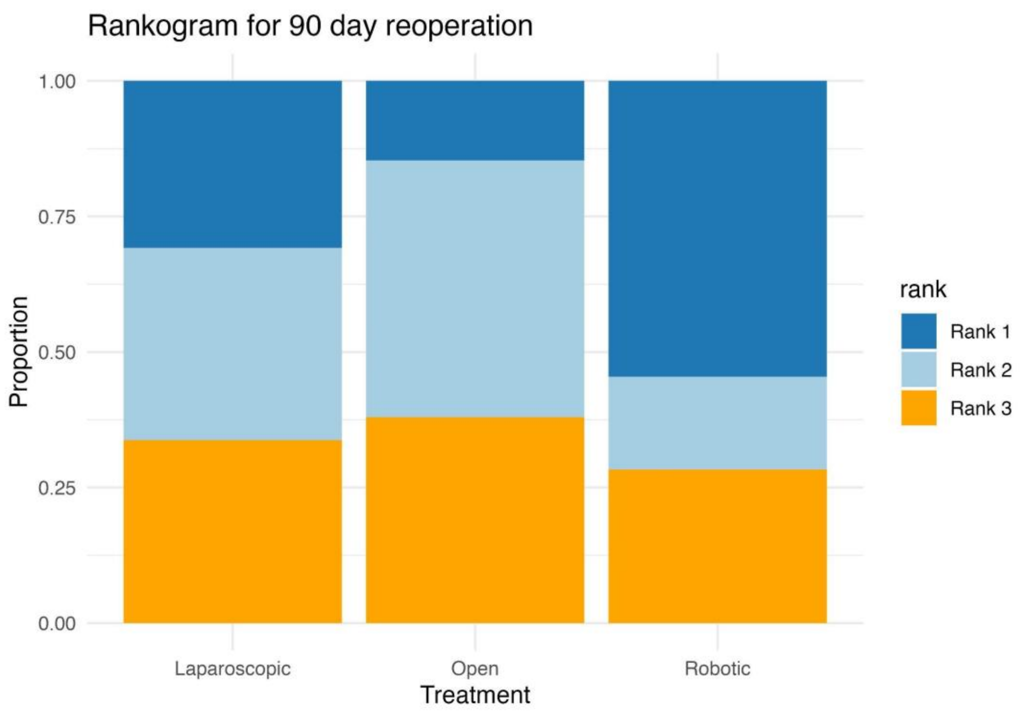

Estimated intraoperative blood loss

Figure 16. network graph Intraoperative blood loss

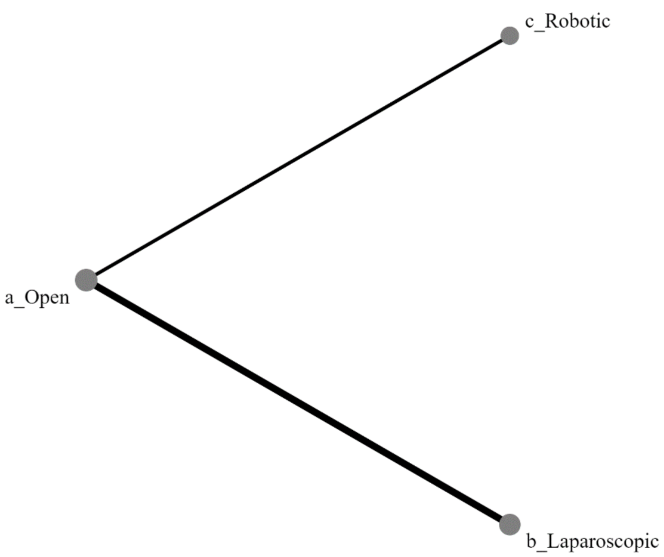

Table 10. Comparison of the included interventions: mean difference (95% CrI). Each cell gives the effect of the column-defining intervention relative to the row-defining intervention.

a_Open	-128.099 (-252.897, -37.312)	-89.434 (-260.938, 86.025)
	b_Laparoscopic	39.484 (-153.153, 266.664)
		c_Robotic

Figure 17. forest plot for intraoperative blood loss

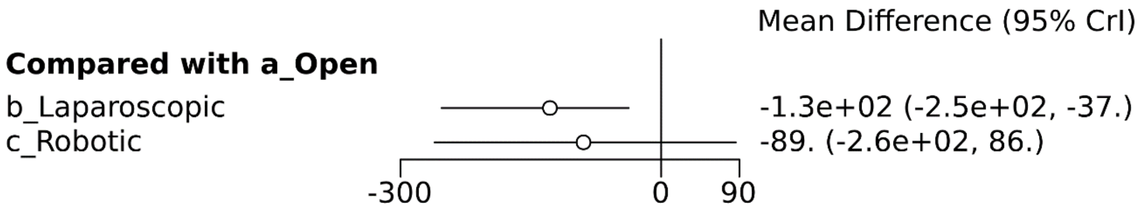

Table 11. Rank probabilities table

	Rank 1	Rank 2	Rank 3
a_Open	0.002	0.117	0.881
b_Laparoscopic	0.711	0.280	0.009
c_Robotic	0.287	0.603	0.110

Figure 18. rankogram for intraoperative blood loss

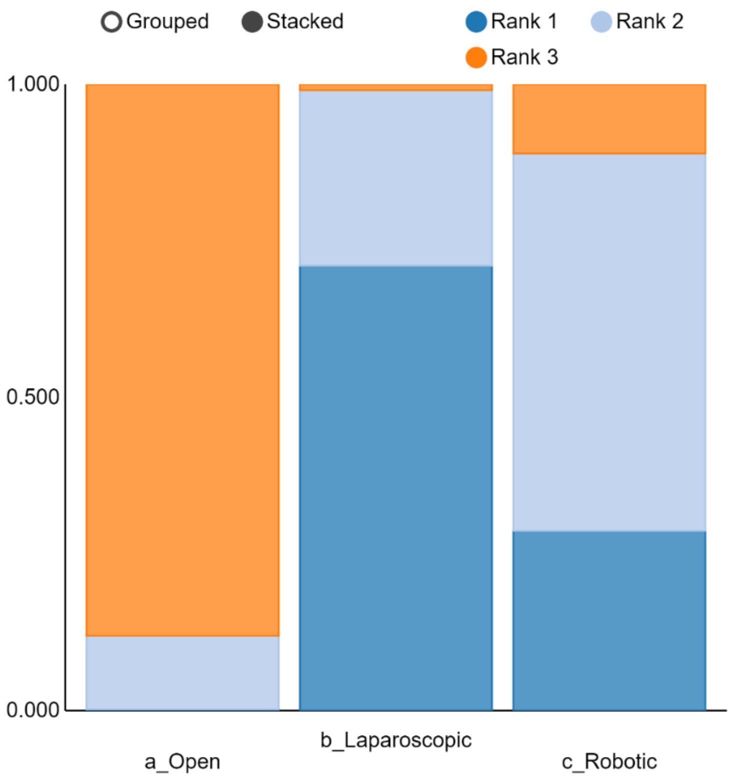

Duration of surgery

Figure 19. Network graph for duration of surgery

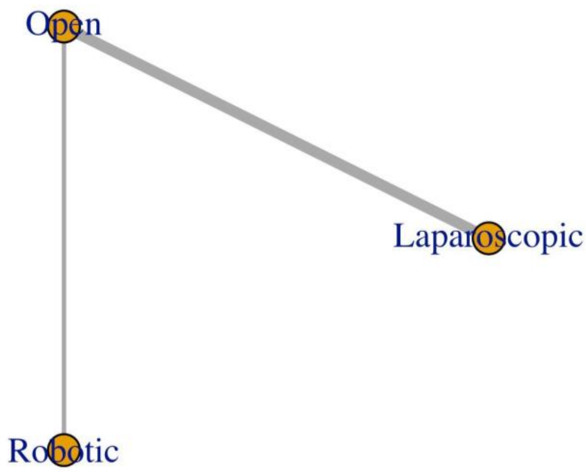

Figure 20. forest plot for duration of surgery

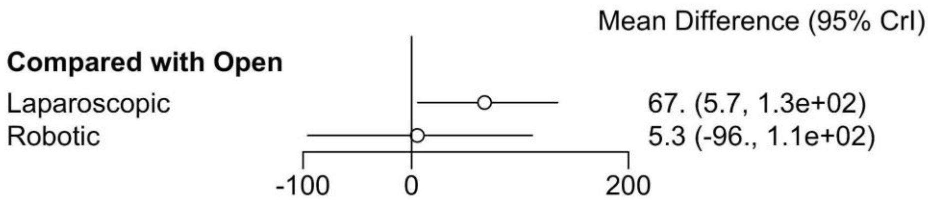

Figure 21.

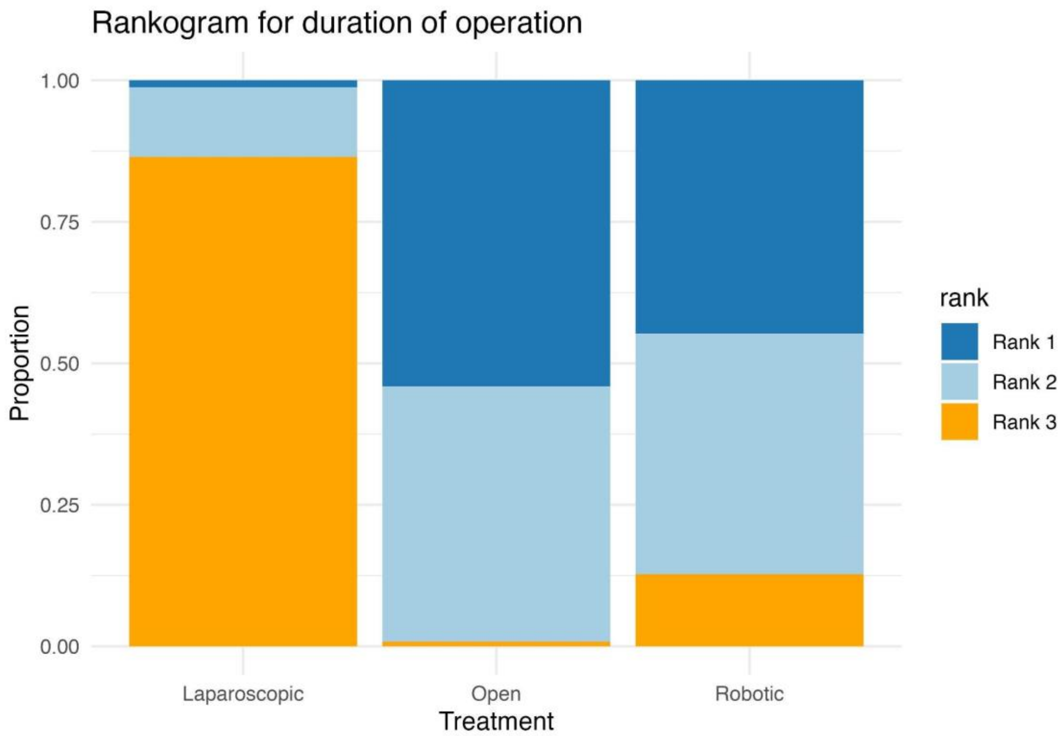
Rankogram for duration of operation
1.00
0.75
0.50
0.25
0.00
Proportion
Laparoscopic
Open
Robotic
Treatment
rank
Rank 1
Rank 2
Rank 3

Postoperative pancreatic fistula

Figure 22. Network graph for postoperative pancreatic fistula

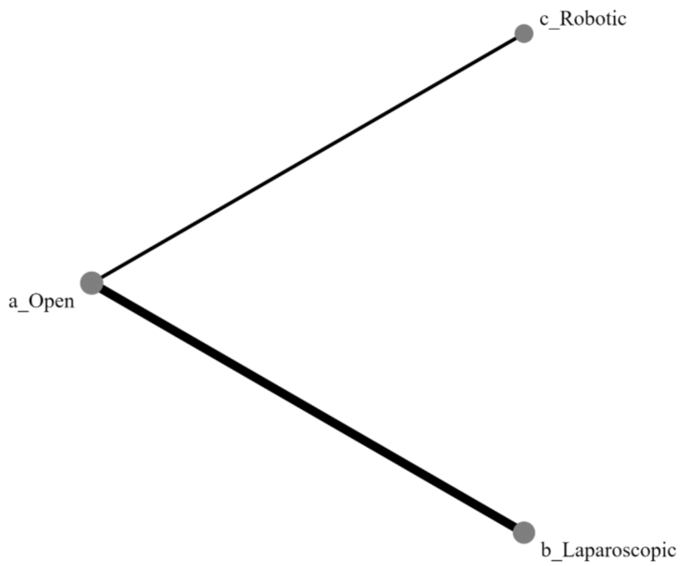

Table 12. Comparison of the included interventions: odds ratio (95% CrI). Each cell gives the effect of the column-defining intervention relative to the row-defining intervention.

a_Open	0.780 (0.425, 1.308)	1.513 (0.624, 3.735)
	b_Laparoscopic	1.961 (0.701, 5.758)
		c_Robotic

Figure 23. forest plot for postoperative fistula

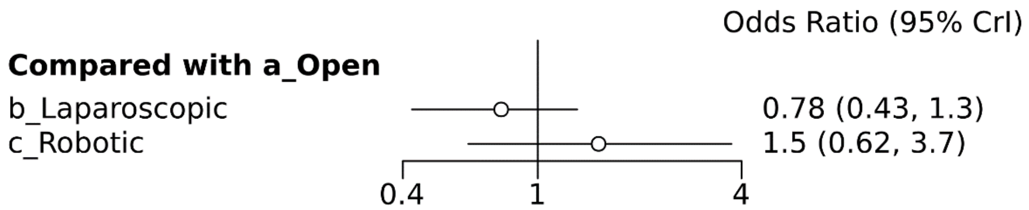

Table 13. Rank probabilities table

	Rank 1	Rank 2	Rank 3
a_Open	0.139	0.723	0.139
b_Laparoscopic	0.781	0.172	0.047
c_Robotic	0.080	0.105	0.815

Figure 24. Rankogram for postoperative pancreatic fistula

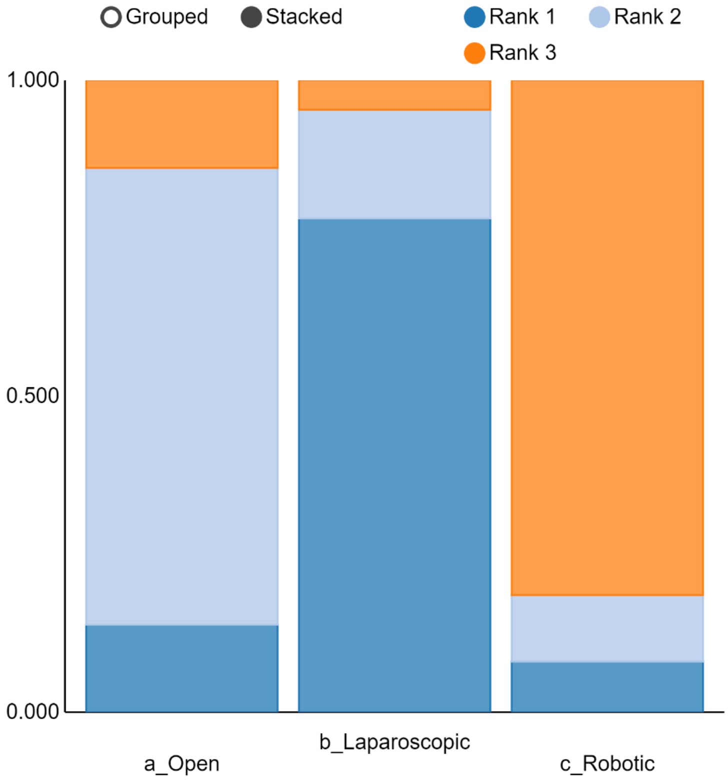

Delayed gastric emptying

Figure 25. Network graph for delayed gastric emptying

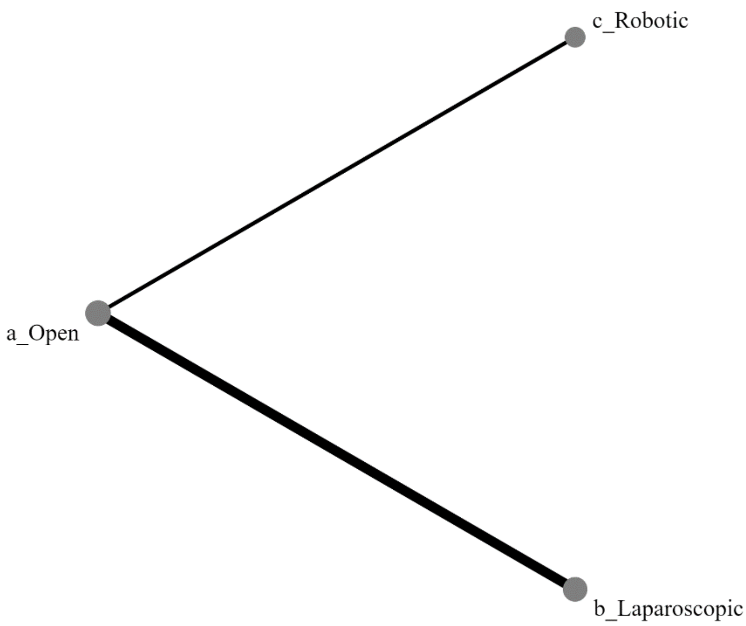

Table 14. Comparison of the included interventions: odds ratio (95% CrI). Each cell gives the effect of the column-defining intervention relative to the row-defining intervention.		
a_Open	0.884 (0.321, 2.223)	2.048 (0.466, 12.154)
	b_Laparoscopic	2.334 (0.407, 19.490)
		c_Robotic

Figure 26. Forrest plot for delayed gastric emptying

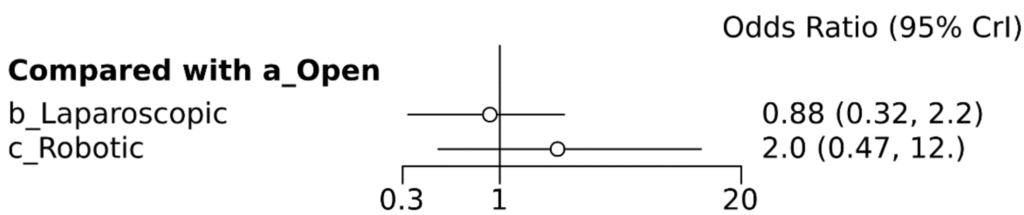

Table 15. Rank probabilities table			
	Rank 1	**Rank 2**	**Rank 3**
a_Open	0.320	0.592	0.089
b_Laparoscopic	0.582	0.320	0.098
c_Robotic	0.099	0.088	0.813

Figure 27. Rankogram for delayed gastric emptying

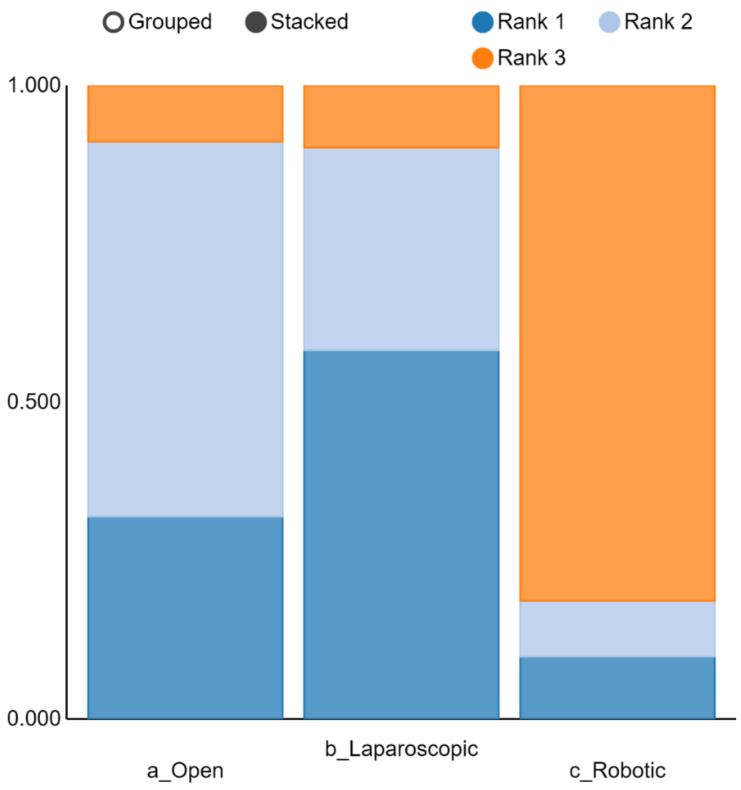

Bile leak

Figure 28. Network graph for bile leak

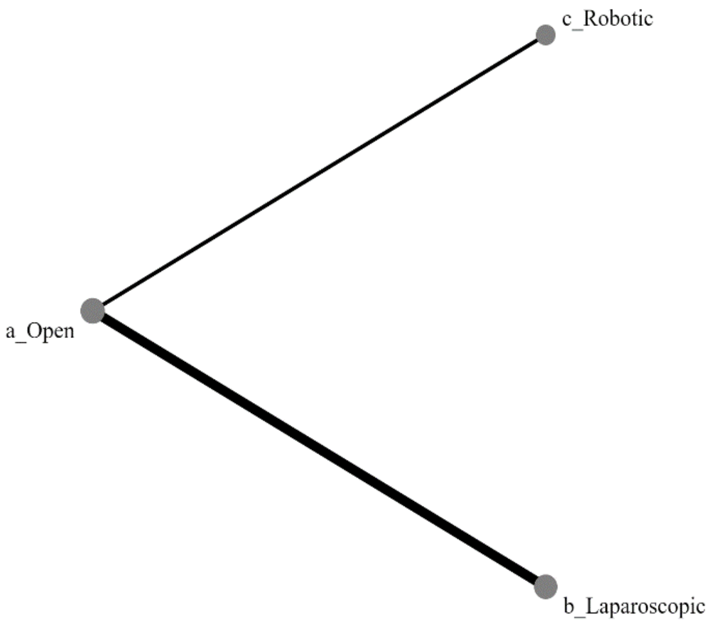

Table 16. Comparison of the included interventions: odds ratio (95% CrI). Each cell gives the effect of the column-defining intervention relative to the row-defining intervention.

a_Open	1.044 (0.486, 2.157)	1.058 (0.308, 3.829)
	b_Laparoscopic	1.008 (0.246, 4.525)
		c_Robotic

Figure 29. Forest plot for bile leak

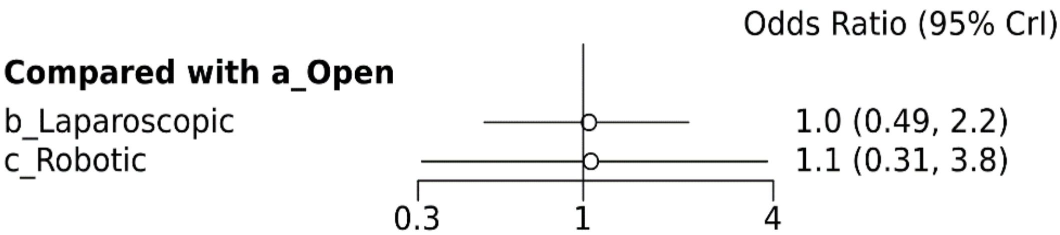

Table 17. Rank probabilities table

	Rank 1	Rank 2	Rank 3
a_Open	0.304	0.483	0.214
b_Laparoscopic	0.303	0.347	0.350
c_Robotic	0.394	0.170	0.436

Figure 30. Rankogram for bile leak

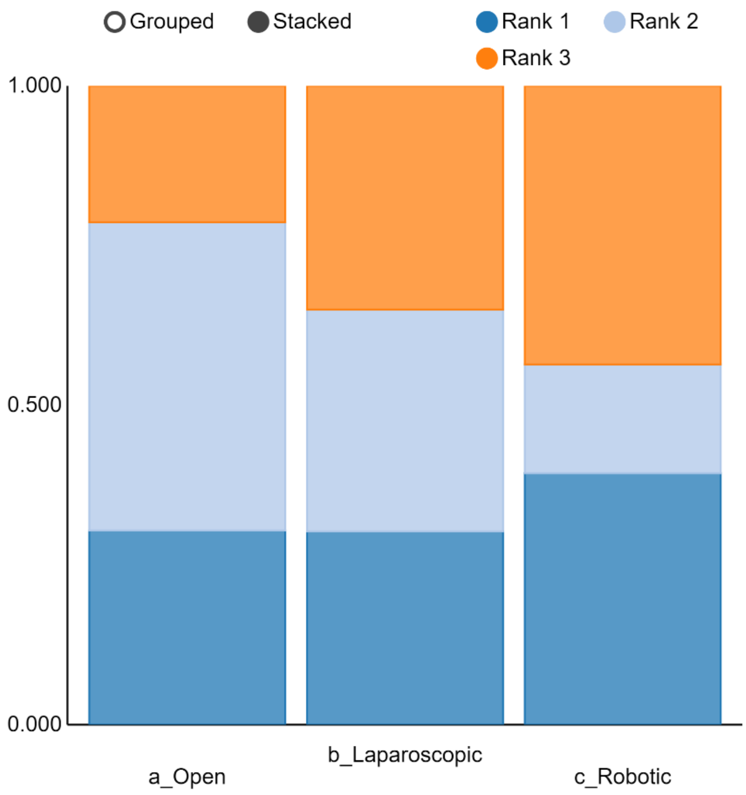

Post-pancreaticoduodenectomy haemorrhage

Figure 31. Network graph for post-pancreatoduodenectomy haemorrhage

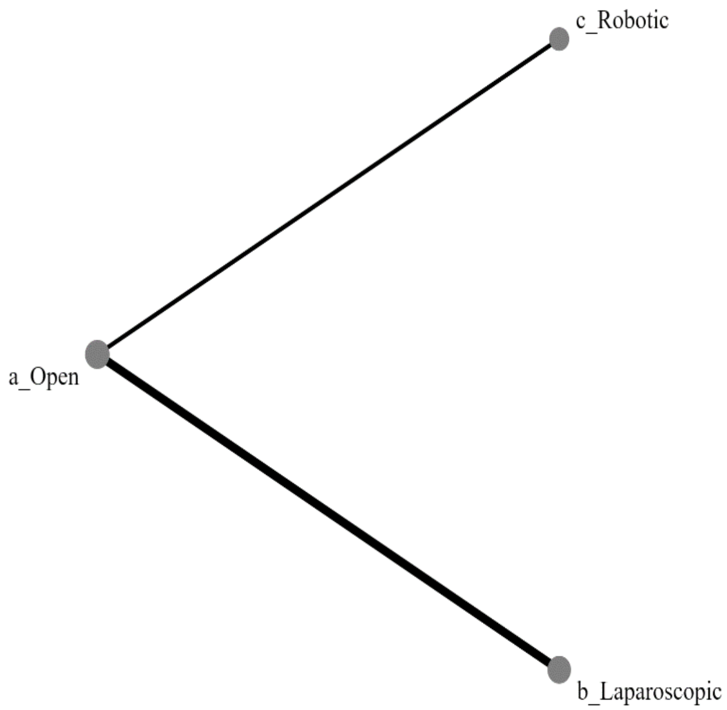

Table 18. Comparison of the included interventions: odds ratio (95% CrI). Each cell gives the effect of the column-defining intervention relative to the row-defining intervention.

a_Open	0.845 (0.341, 1.902)	1.257 (0.379, 5.558)
	b_Laparoscopic	1.487 (0.372, 9.055)
		c_Robotic

Figure 32. Forest plot for post-pancreatoduodenectomy haemorrhage

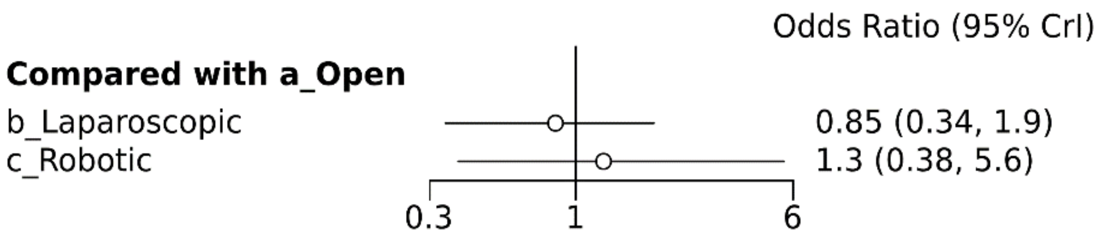

Table 19. Rank probabilities table

	Rank 1	Rank 2	Rank 3
a_Open	0.209	0.556	0.236
b_Laparoscopic	0.558	0.284	0.158
c_Robotic	0.234	0.161	0.606

Figure 33. Rankogram for post-pancreatoduodenectomy haemorrhage

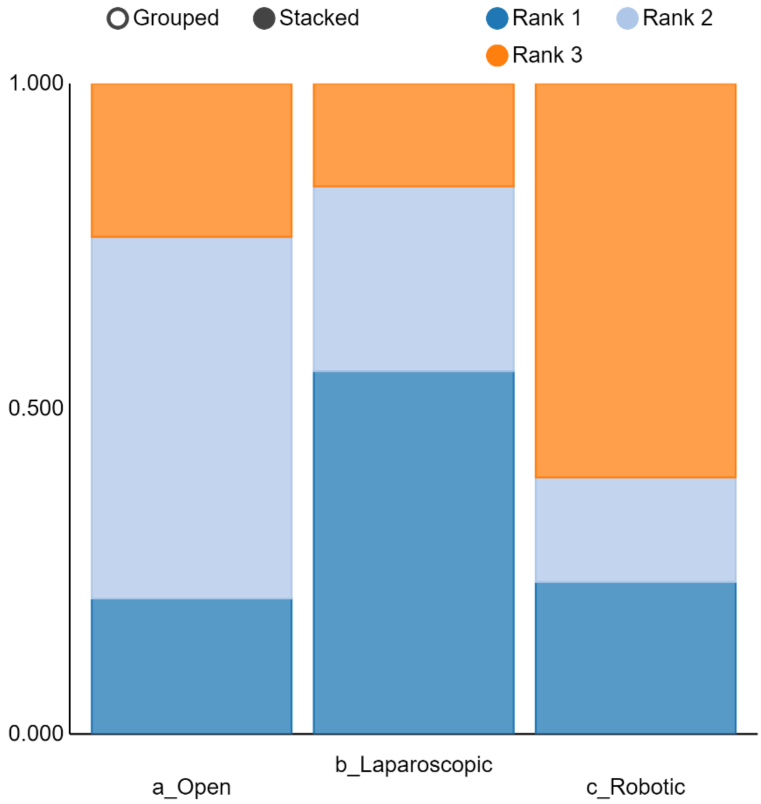

Oncological outcome

Number of lymph nodes resected

Figure 34. Network graph for number of nodes resected

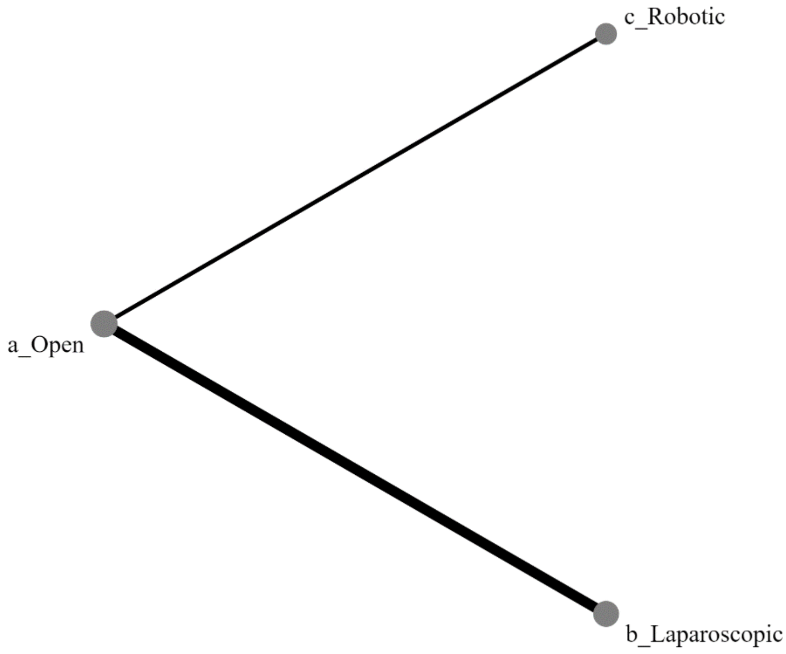

Table 20. Comparison of the included interventions: mean difference (95% CrI). Each cell gives the effect of the column-defining intervention relative to the row-defining intervention.

a_Open	1.170 (-1.681, 4.632)	1.271 (-3.506, 6.866)
	b_Laparoscopic	0.090 (-6.079, 6.265)
		c_Robotic

Figure 35. Forest plot for number of nodes resected

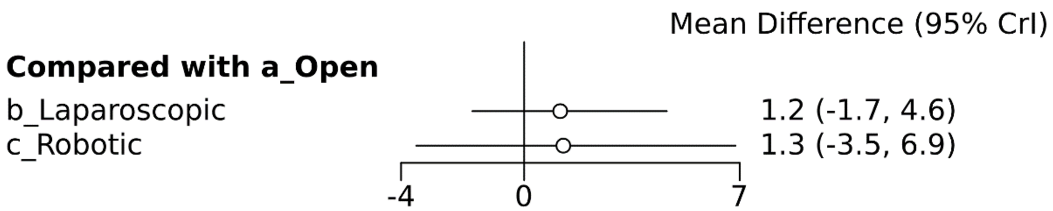

Table 21. Rank probabilities table

	Rank 1	Rank 2	Rank 3
a_Open	0.045	0.330	0.624
b_Laparoscopic	0.454	0.418	0.129
c_Robotic	0.501	0.252	0.247

Figure 36. Network graph for number of nodes resected

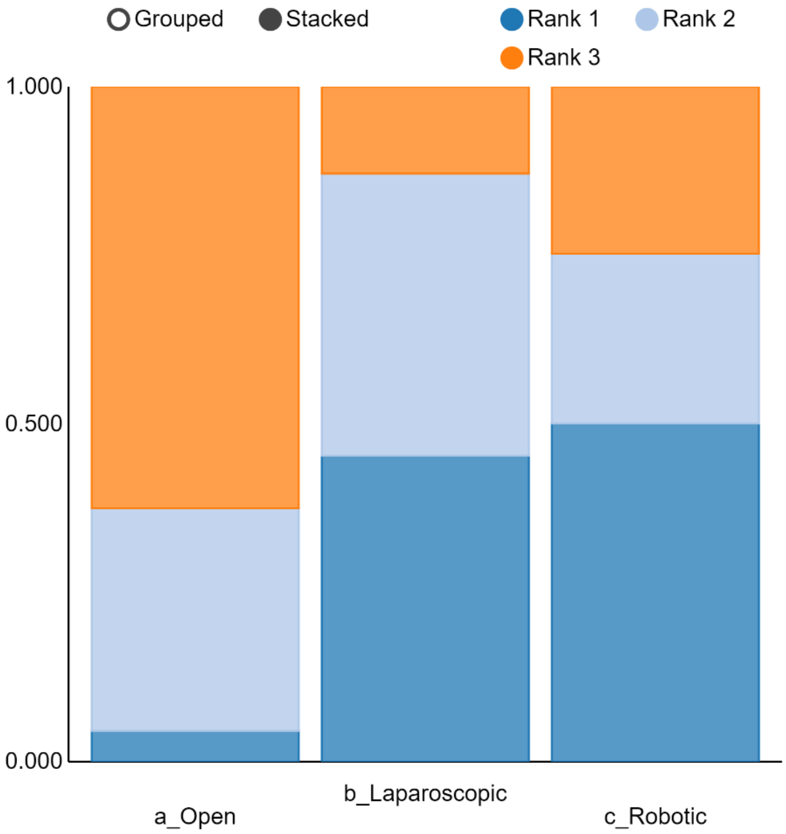

Heterogeneity Analysis

Postoperative length of stay

Some heterogeneity (Random effects standard deviation 1.577 (95% CrI 0.079, 8.280)). Node-splitting inconsistency value was not produced due to insufficient trial arms and studies to produce robust values.

Estimated intraoperative blood loss

Some heterogeneity (Random effects standard deviation 69.505 (95% CrI 21.269, 226.371)). Node-splitting inconsistency value was not produced due to insufficient trial arms and studies to produce robust values.

Postoperative 90-day mortality

Some heterogeneity (Random effects standard deviation 1.257 (95% CrI 0.130, 1.911). Node-splitting inconsistency value was not produced due to insufficient trial arms and studies to produce robust values.

Postoperative 90-day readmission

No heterogeneity was found (Random effects standard deviation 0.411 (0.016, 1.444)). Node-splitting inconsistency value was not produced due to insufficient trial arms and studies to produce robust values.

Postoperative 90-day reoperation

No heterogeneity was found (Random effects standard deviation 0.553 (95% CrI 0.027, 1.446)). Node-splitting inconsistency value was not produced due to insufficient trial arms and studies to produce robust values.

POPF

No heterogeneity was found (Random effects standard deviation 0.260 (95% CrI 0.012, 0.833)). Node-splitting inconsistency value was not produced due to insufficient trial arms and studies to produce robust values.

DGE

Some heterogeneity (Random effects standard deviation 0.787 (95% CrI 0.081, 1.760)). Node-splitting inconsistency value was not produced due to insufficient trial arms and studies to produce robust values.

Biliary leak

Some heterogeneity (Random effects standard deviation 70.555 (95% CrI 21.421, 225.915)). Node-splitting inconsistency value was not produced due to insufficient trial arms and studies to produce robust values.

PPH

No heterogeneity was found (Random effects standard deviation 0.454 (95% CrI 0.023, 1.250)). Node-splitting inconsistency value was not produced due to insufficient trial arms and studies to produce robust values.

Number of nodes resected

Some heterogeneity (Random effects standard deviation 1.537 (95% CrI 1.201, 2.018)). Node-splitting inconsistency value was not produced due to insufficient trial arms and studies to produce robust values.

Pairwise meta-analysis

Figure 36. Length of stay (laparoscopic PD vs open PD)

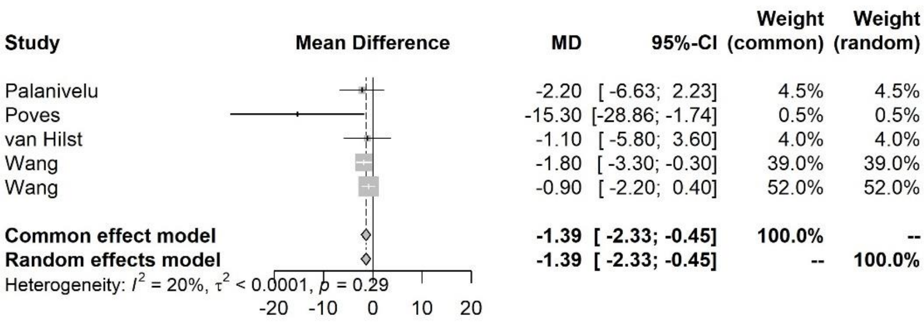

Figure 37. 90-day mortality (laparoscopic PD vs open PD)

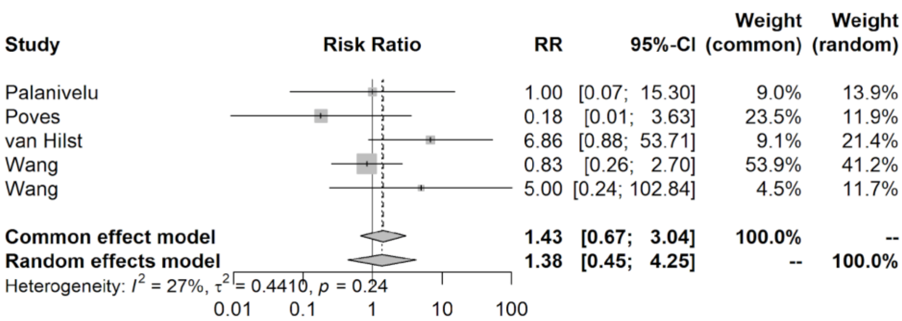

Figure 38. 90-day readmission (laparoscopic PD vs open PD)

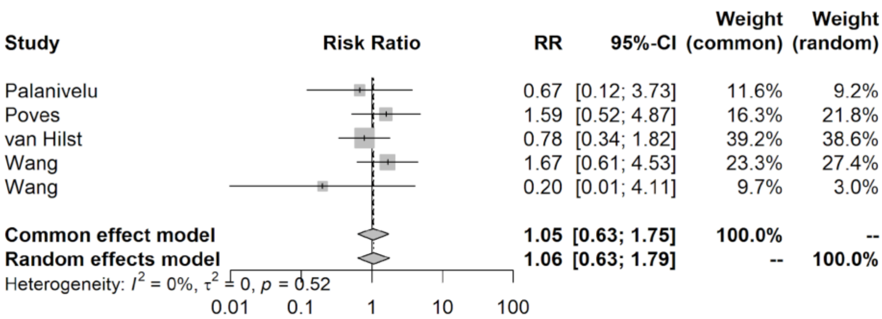

Figure 39. 90-day reoperation (laparoscopic PD vs open PD)

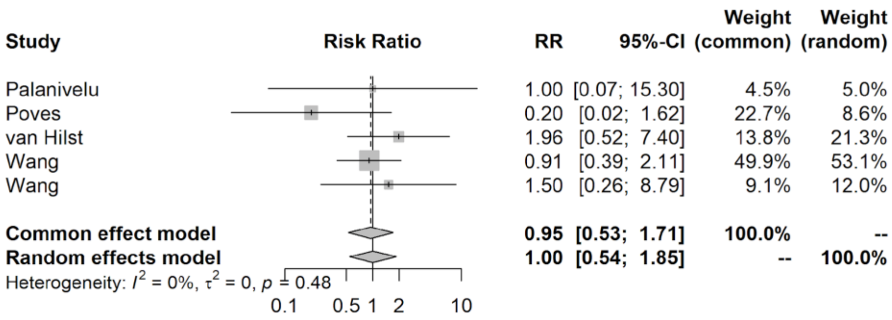

Figure 40. Intraoperative blood loss (laparoscopic PD vs open PD)

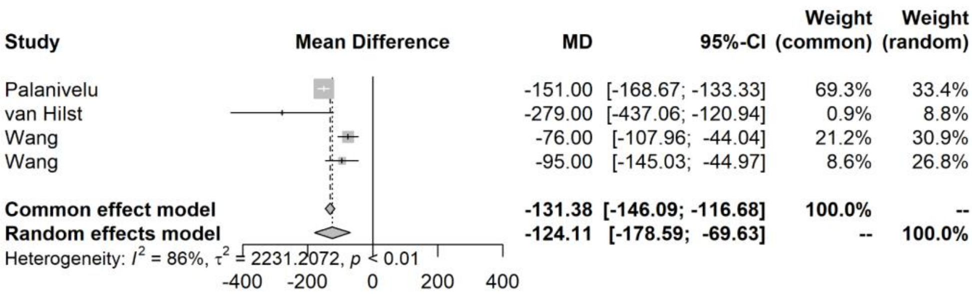

Figure 41. Duration of surgery (laparoscopic PD vs open PD)

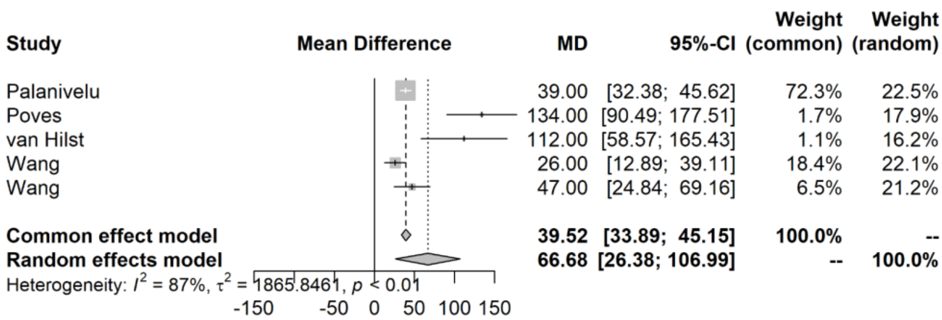

Figure 42. POPF (laparoscopic PD vs open PD)

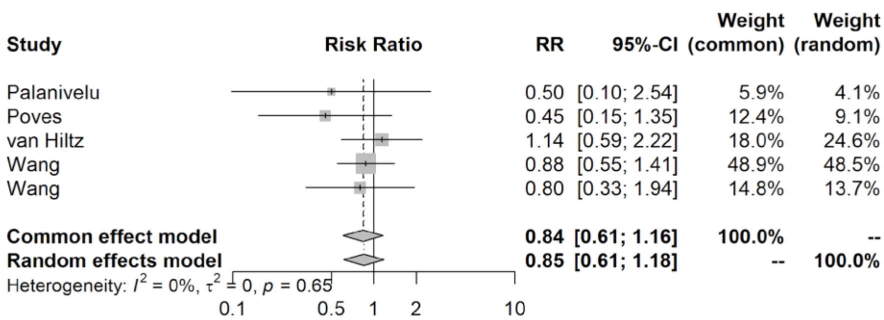

Figure 43. Bile leak (laparoscopic PD vs open PD)

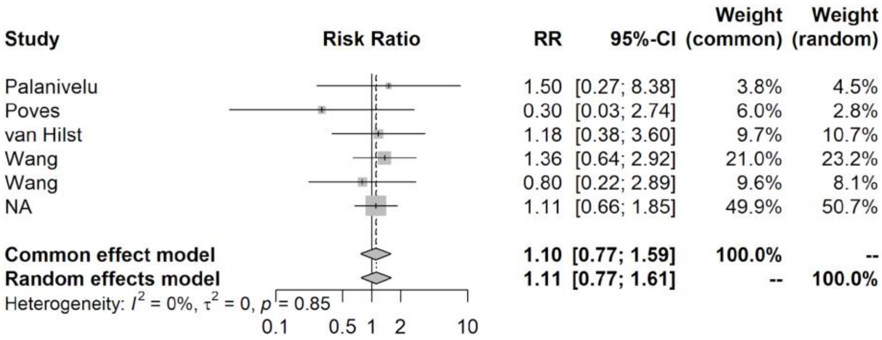

Figure 44. DGE (laparoscopic PD vs open PD)

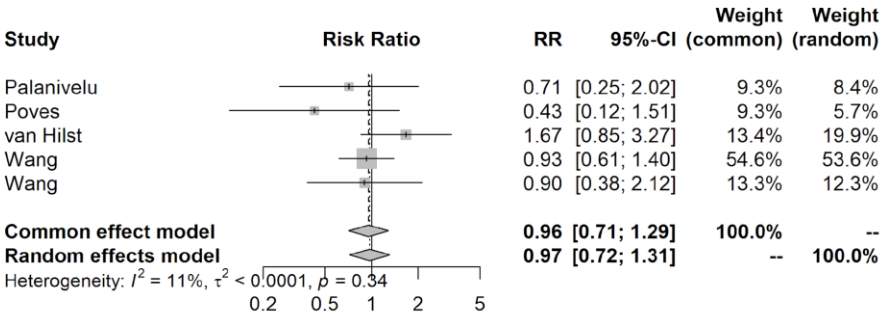

Figure 45. PPH (laparoscopic PD vs open PD)

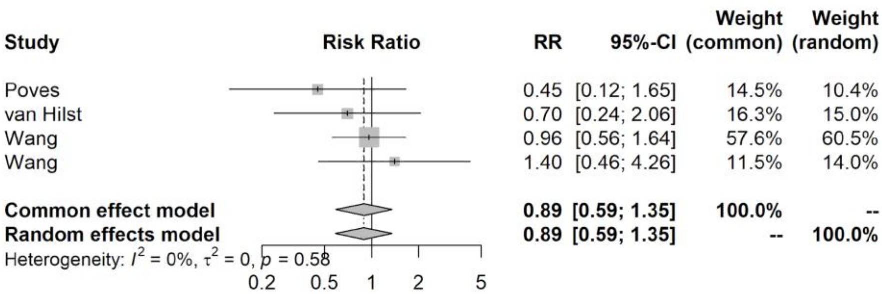

Figure 46. Number of nodes retrieved (laparoscopic PD vs open PD)

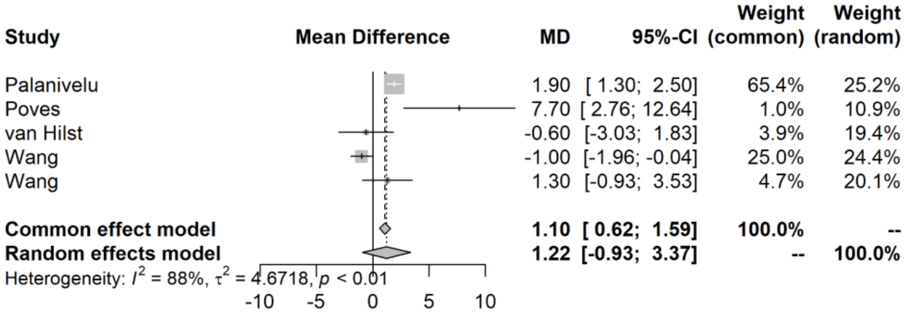

Figure 47. Length of stay (robotic PD vs open PD)

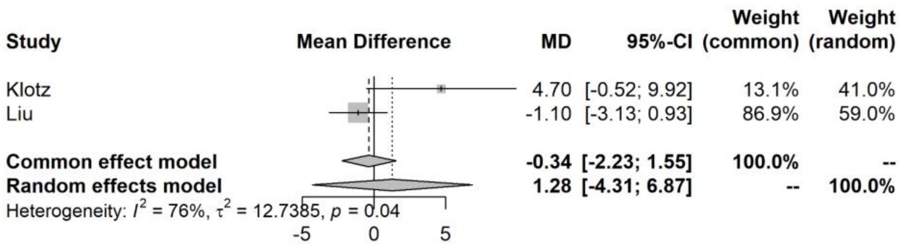

Figure 48. 90-day mortality (robotic PD vs open PD)

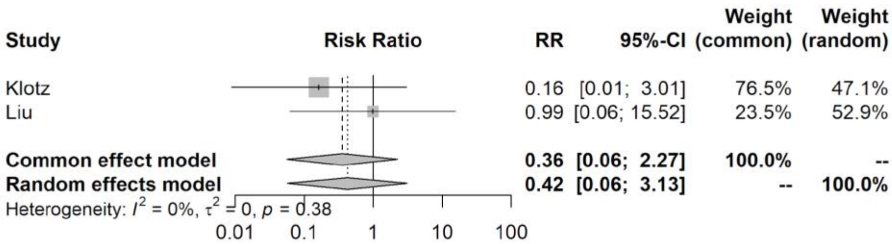

Figure 49. 90-day readmission (robotic PD vs open PD)

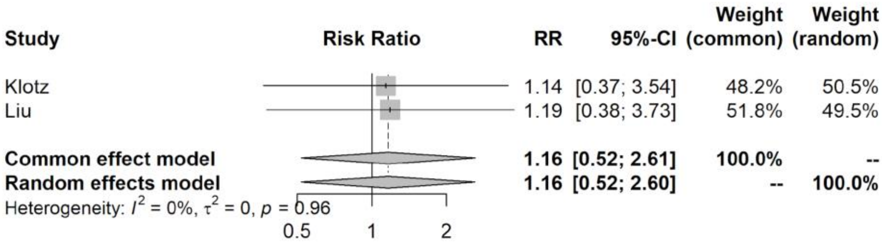

Figure 50. 90-day reoperation (robotic PD vs open PD)

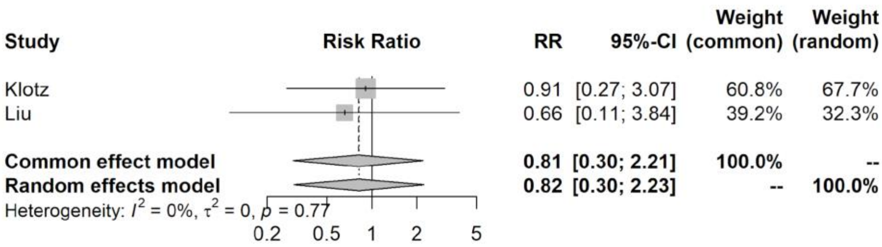

Figure 51. Intraoperative blood loss (robotic PD vs open PD)

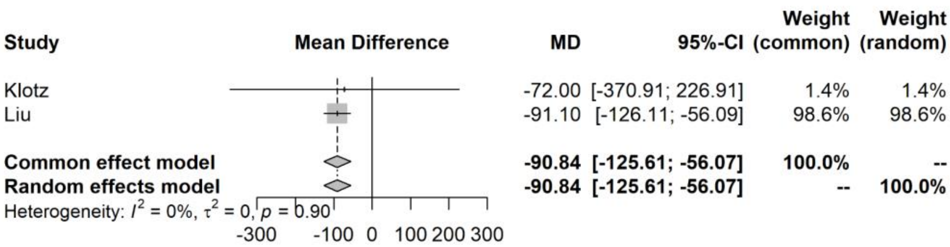

Figure 52. Duration of surgery (robotic PD vs open PD)

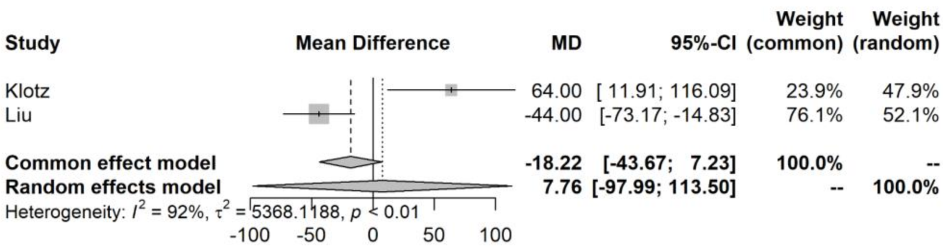

Figure 52. POPF (robotic PD vs open PD)

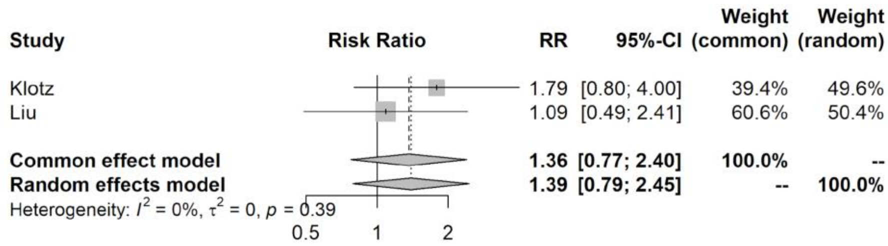

Figure 53. Bile leak (robotic PD vs open PD)

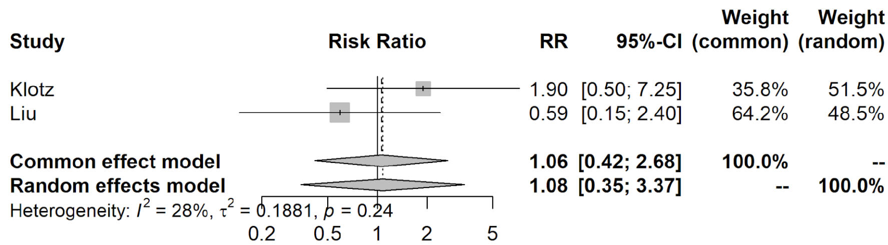

Figure 54. DGE (robotic PD vs open PD)

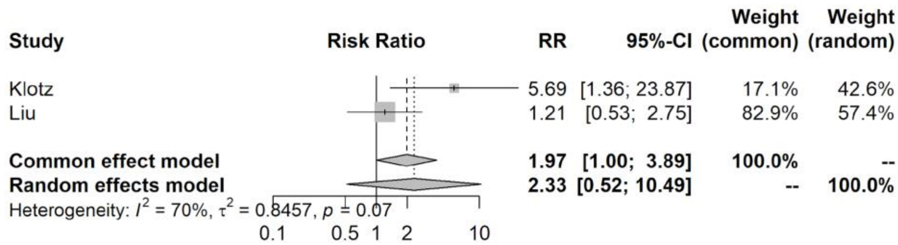

Figure 55. PPH (robotic PD vs open PD)

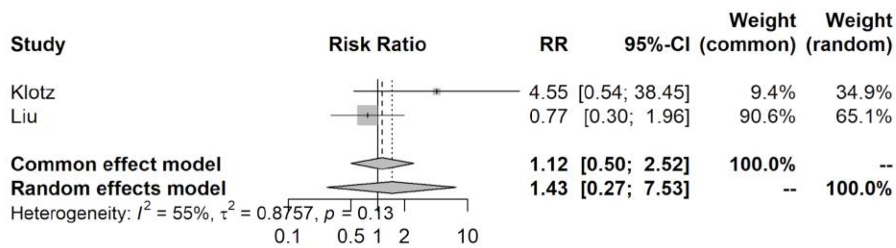

Figure 56. Number of nodes retrieved (robotic PD vs open PD)

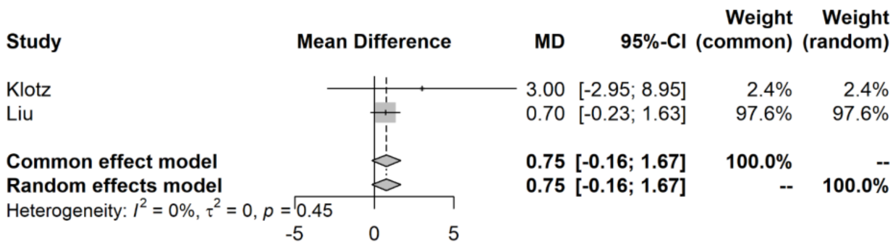

Trial sequential analysis

Figure 57. TSA plot for length of stay (laparoscopic PD vs open PD)

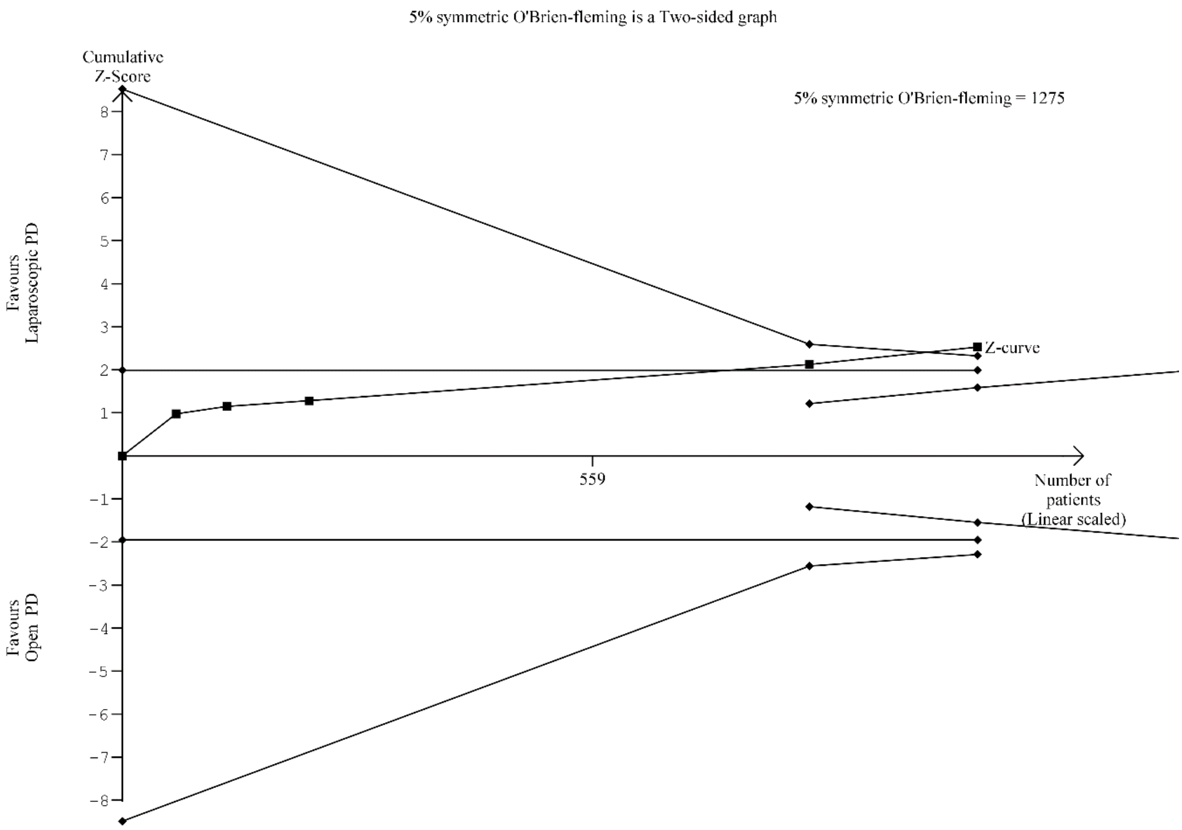

Figure 58. TSA plot for 90-day mortality (laparoscopic PD vs open PD)

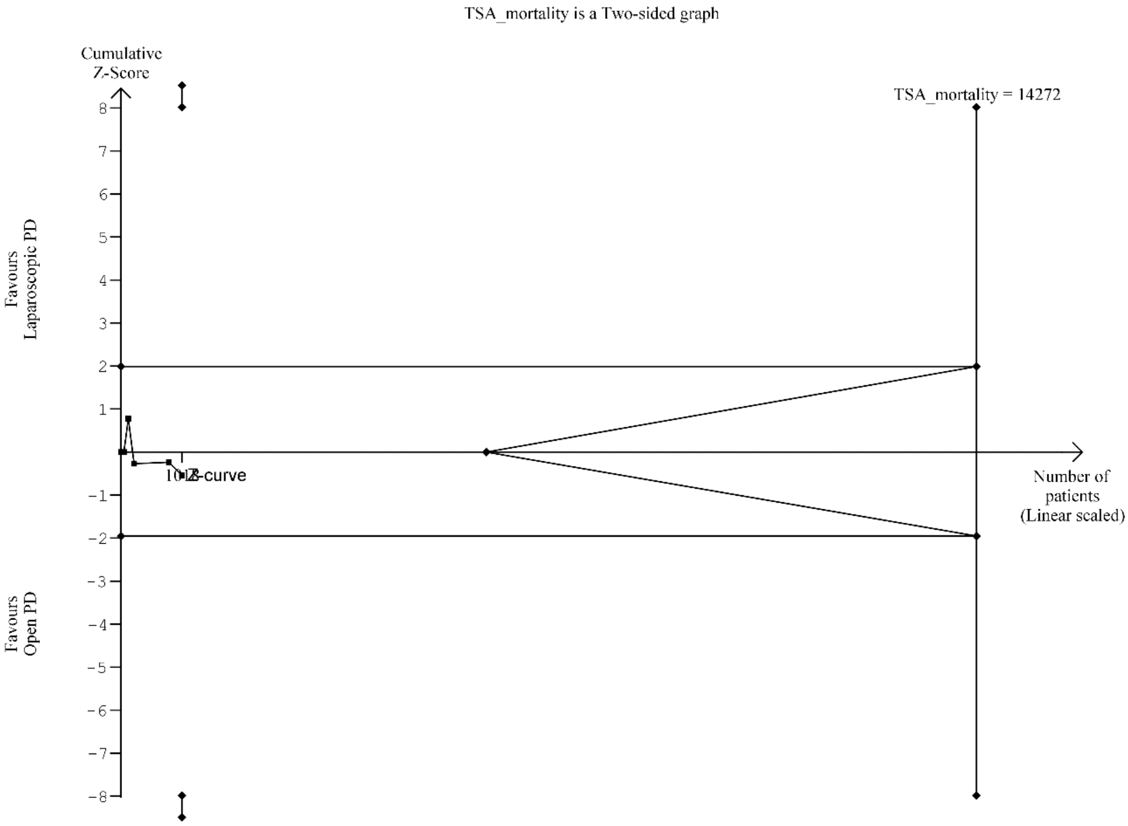

Figure 59. TSA plot for POPF (laparoscopic vs open PD)

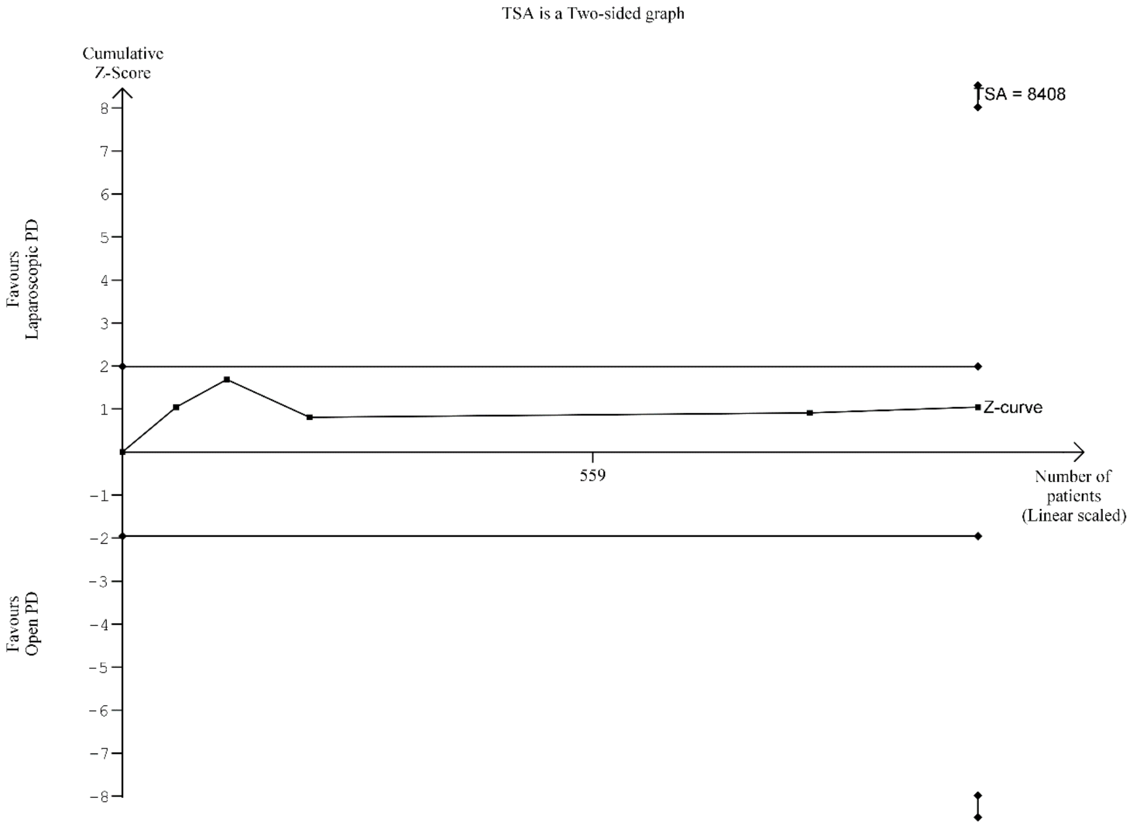

Figure 60. TSA plot for length of surgery (laparoscopic vs open)

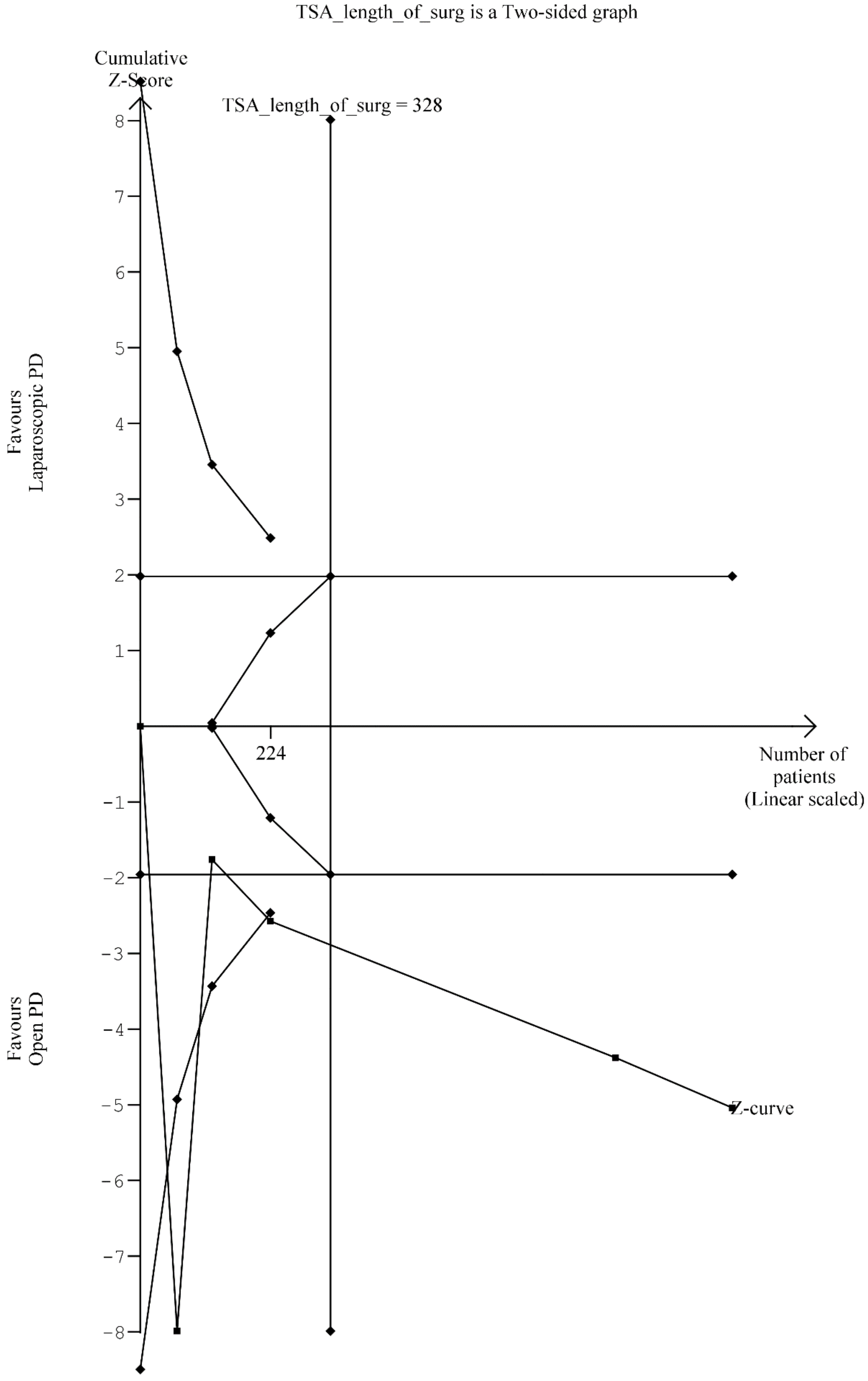

Figure 61. TSA plot for number of nodes retrieved (laparoscopic vs open)

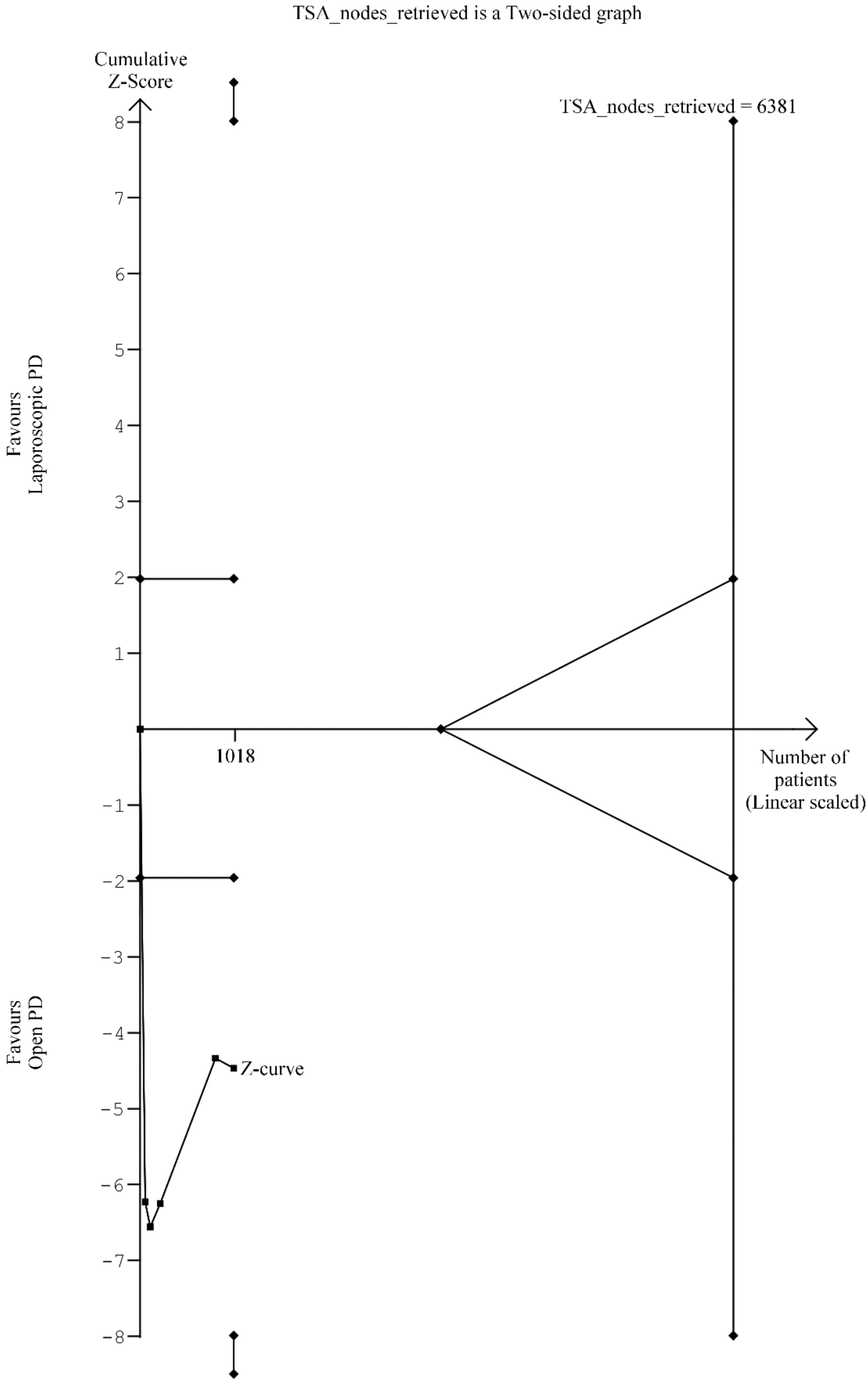

Figure 62. TSA plot for 90-day mortality (robotic PD vs open PD)

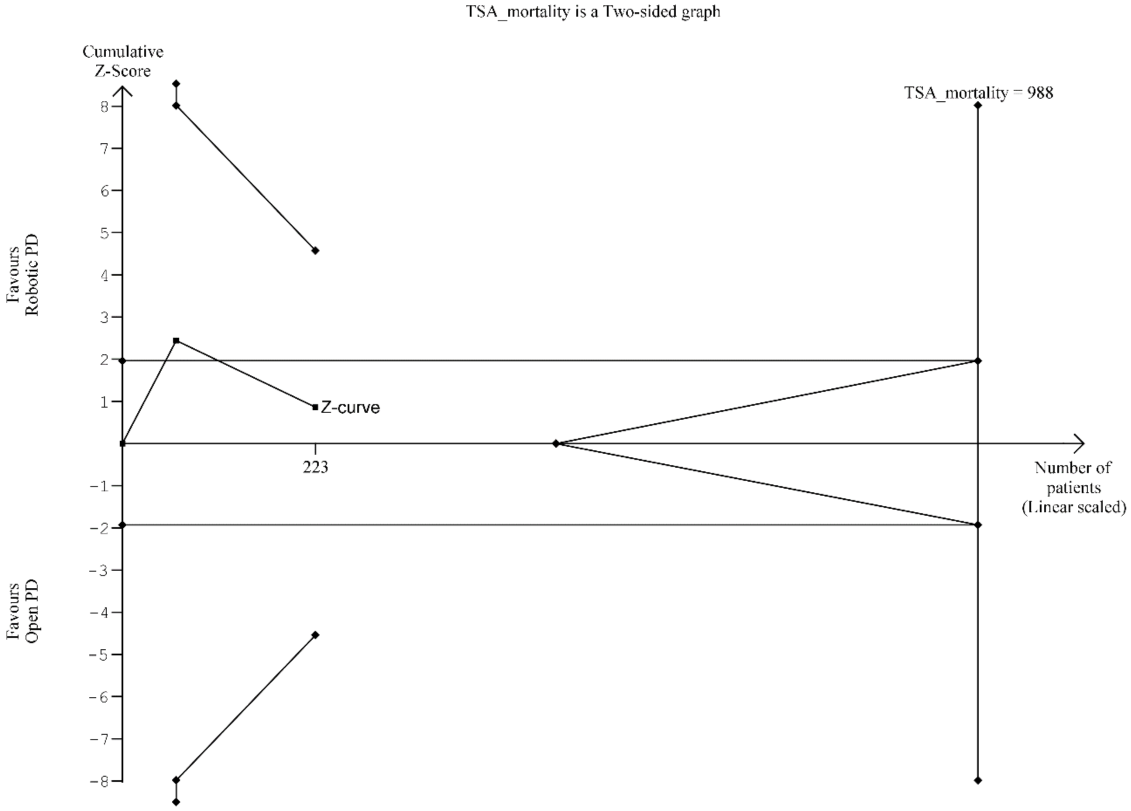

Figure 63. TSA plot for number of nodes retrieved (robotic vs open PD)